SUPPLEMENTARY FIGURES AND LEGENDS

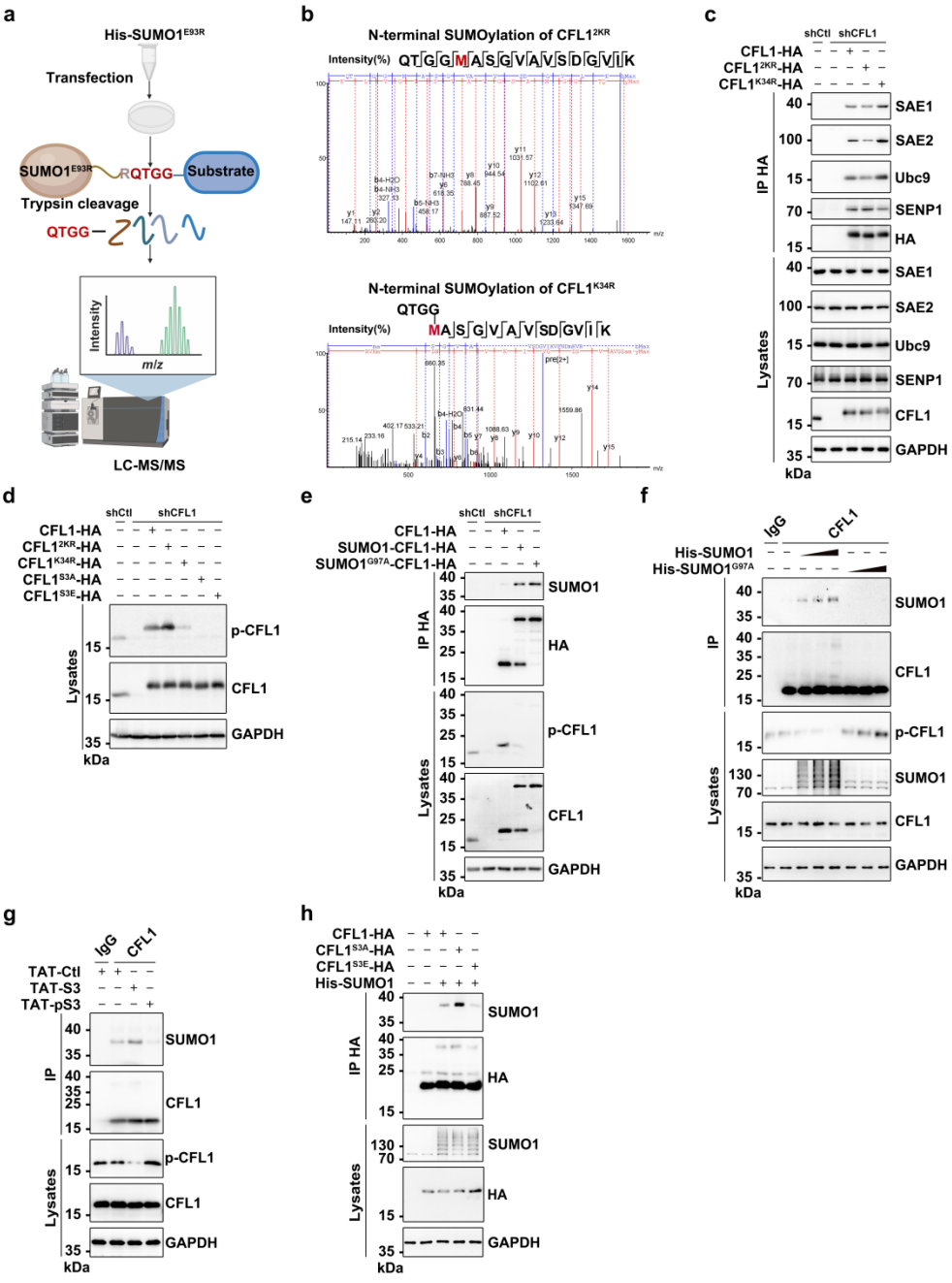

Supplementary Figure 1. The inhibition between SUMOylation and phosphorylation of CFL1. a Diagram illustrating CFL1 SUMOylation identification using IP-MS. HEK 293T cells with endogenous CFL1 knocked down were co-transfected CFL1^{2KR}-HA or CFL1^{K34R}-HA and His-SUMO1^{E93R} plasmids. De-IP with anti-HA beads. IP products underwent trypsin digestion and LC-MS/MS analysis. Created in BioRender. Weng, W. (2025) https://BioRender.com/8l7vzuc. **b** MS/MS spectrum of a tryptic peptide containing glutamine-threonine-glycine-glycine (QTGG) preceding the N-terminal methionine of CFL1^{2KR}-HA and CFL1^{K34R}-HA, determined by collision-activated dissociation. **c** CFL1^{K34R} exhibited enhanced binding to SAE1/SAE2 and Ubc9, but decreased binding to SENP1. HEK 293T cells with endogenous CFL1 knocked down, overexpression of CFL1-HA, CFL1^{2KR}-HA, or CFL1^{K34R}-HA. Co-IP with anti-HA beads, followed by WB. **d** HEK 293T cells with endogenous CFL1 knocked down, overexpression of CFL1-HA, CFL1^{2KR}-HA, CFL1^{K34R}-HA, CFL1^{S3A}-HA or CFL1^{S3E}-HA. CFL1^{2KR} exhibited increased phosphorylation. CFL1^{K34R} exhibited decreased phosphorylation. **e** Overexpression of His-SUMO1 in CHO-K1 cells resulted in increased SUMOylation and decreased phosphorylation. In contrast, overexpression of His-SUMO1^{G97A} led to decreased SUMOylation and increased phosphorylation. **f** Expressing either SUMO-CFL1 or SUMO1^{G97A}-CFL1 in HEK 293T cells with stable of endogenous CFL1 knocked down exhibited decreased phosphorylation. **g** CHO-K1 cells treated with TAT-S3 peptide (10 μM, 16 h) exhibited increased SUMOylation and decreased phosphorylation, cells treated with TAT-pS3 peptide exhibited decreased SUMOylation and increased phosphorylation. IP with control IgG or anti-CFL1 antibody followed by WB. **h** CHO-K1 cells expressed CFL1^{S3A}-HA and His-SUMO1 exhibited increased SUMOylation. In contrast, CFL1^{S3E}-HA exhibited decreased SUMOylation. Source data are provided as a Source Data file.

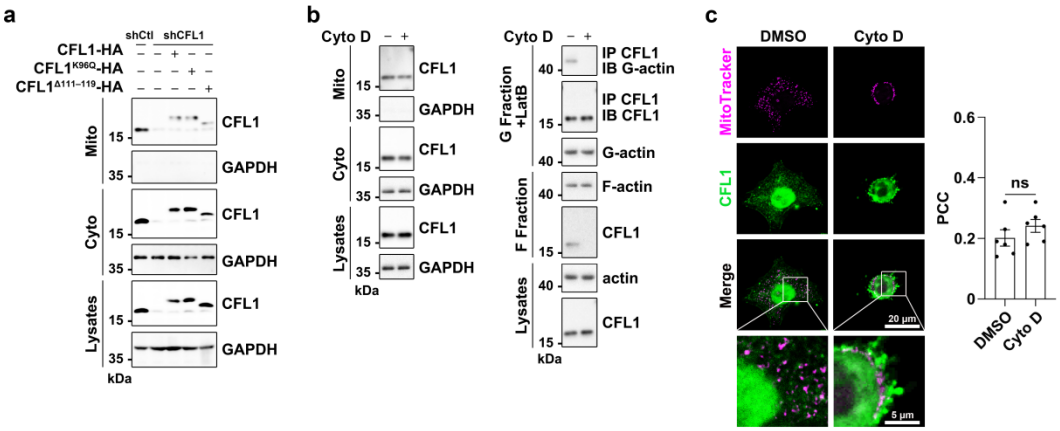
a
shCtl
shCFL1
CFL1-HA
CFL1K96Q-HA
CFL1Δ111–119-HA
Mito
Cyto
Lysates
CFL1
GAPDH
15
35
kDa
b
Cyto D
Mito
Cyto
Lysates
CFL1
GAPDH
G Fraction +LatB
F Fraction
IP CFL1
IB G-actin
IP CFL1
IB CFL1
G-actin
F-actin
actin
40
c
DMSO
Cyto D
MitoTracker
CFL1
Merge
20 μm
5 μm
PCC
ns
0.6
0.4
0.2
0

Supplementary Figure 2. Inhibiting the interaction between CFL1 and F-actin or G-actin does not affect CFL1 mitochondrial translocation. a Overexpression of F-actin binding site mutation ($CFL1^{K96Q}$-HA) or G-actin binding region deletion mutation ($CFL1^{\Delta 111-119}$-HA) in HEK 293T cells with endogenous CFL1 knocked down had no impact on CFL1 mitochondrial translocation. **b** Inhibiting the interaction between CFL1 and F-actin or G-actin by Cyto D had no impact on CFL1 mitochondrial translocation. HEK 293T cells treated with Cyto D (10 μM, 6 h) and then Isolated G-actin and F-actin. The supernatant fraction containing G-actin was treated with Lat B (10 μM) to inhibit G-actin polymerization, followed by Co-IP with anti-CFL1 antibody for 12 h. Mito, Cyto or total lysates fractions were prepared from the same cells, followed by WB. **c** Confocal images of colocalization between CFL1 and mitochondria in HeLa cells treated with Cyto D. The PCC was presented as the mean ± SEM of six visual fields from 3 biological replicates; “ns” ($p = 0.6081$), analyzed by a two-tailed Student’s t-test. Source data are provided as a Source Data file.

a

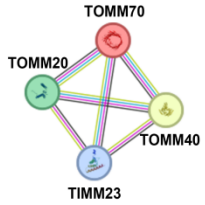

b

Presequence

Possessing mitochondrial presequence (Precision:0.83, Recall:0.73)

Possessing mitochondrial presequence (Precision:0.79, Recall:0.80)

No mitochondrial presequence

Cleavage site

MPP cleavage site

Oct1 cleavage site

Icp55 cleavage site

Motif

TOM20 recognition motif (φχβφφ)

Max positively charged amphiphilicity (PA) score region (high)

Max positively charged amphiphilicity (PA) score region (low)

φ β σ γ Reduced letters composing statistically significant 6mer in presequence

φ(hydrophobic), β(basic), σ(polar), γ(secondary structure breaker)

Protein	Probability of presequence	Cleavage site (processing enzyme)	Net charge	Sequence (100 amino acids from N terminal)
CFL1	0.005	33 MPP	0.121	9 18 1 MASGVAVSDGVIKVFNDMKVRKSSTPEEVKKRK 34 KAVLFCLSEDKKNIILEEGKEILVGDVGQTVDDPY 69 TTFVKMLPDKDCRYALYDATYETKESKKEDLV

c

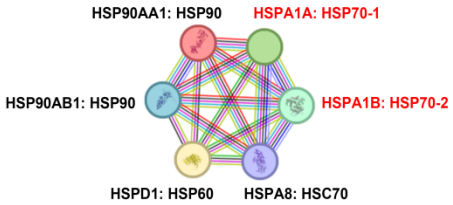

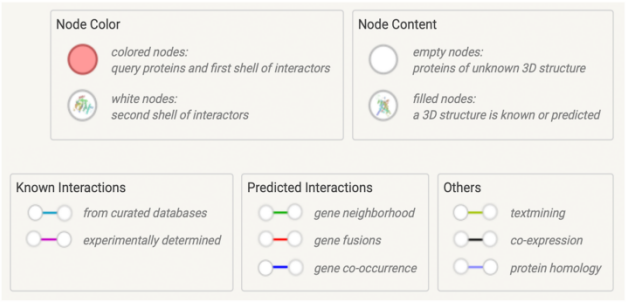

Supplementary Figure 3. Prediction of the mitochondrial translocation mechanism of CFL1. a Protein–protein interaction (PPI) network analysis of Tom and Tim23 complexes using the STRING database. The differential interacting partners were identified by Co-IP/MS performed by expression of CFL1-HA in HEK 293T cells with endogenous CFL1 knocked down. A medium confidence level (0.4) was used. **b** MitoFates was used to predict the mitochondrial targeting sequences of CFL1. **c** The interaction network of heat shock proteins (HSPs) associated with mitochondrial protein import was constructed using the STRING database with a medium confidence score (0.4). The circles represent proteins, while the straight lines represent the interactions between different proteins. The differential interacting partners were identified by Co-IP/MS performed by expression of CFL1-HA in HEK 293T cells with endogenous CFL1 knocked down.

a

Presequence

Possessing mitochondrial presequence (Precision:0.83, Recall:0.73)

Possessing mitochondrial presequence (Precision:0.79, Recall:0.80)

No mitochondrial presequence

Cleavage site

MPP cleavage site

Oct1 cleavage site

Icp55 cleavage site

Motif

TOM20 recognition motif (φχβφφ)

Max positively charged amphiphilicity (PA) score region (high)

Max positively charged amphiphilicity (PA) score region (low)

φ β σ γ Reduced letters composing statistically significant 6mer in presequence

φ(hydrophobic), β(basic), σ(polar), γ(secondary structure breaker)

Protein	Probability of presequence	Cleavage site (processing enzyme)	Net charge	Sequence (100 amino acids from N terminal)
SUMO1-CFL1	0.000	64 MPP	0.031	1 MSDQEAKPSTEDLGDKKEGEYIKLKVIGQDSSEI 34 HFKVKMTTHLKKLKESYCQRQGVPMNSLRFLFE 69 GQRIADNHTPKELGMEEEDVIEVYQEQTGGMAS

b

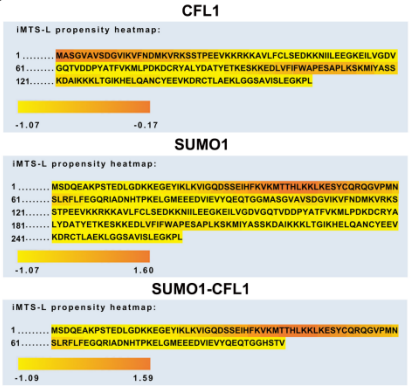

c

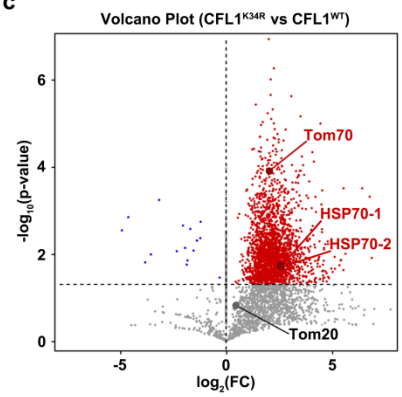

Supplementary Figure 4. Prediction of the mechanism by which CFL1 SUMOylation regulates its mitochondrial translocation. a MitoFates was used to predict the mitochondrial targeting sequences of SUMO1-CFL1. **b** iMLP, a deep learning approach for the prediction of internal matrix targeting-like sequences (iMTS-Ls) was used to predict the iMTS-L propensity scores of CFL1, SUMO1 and SUMO1-CFL1. **c** Volcano plots depicting $\log_2$ fold change and $-\log_{10}$ (p-value) of enriched proteins identified by Co-IP/MS. The adjusted p-value < 0.05, determined by two-tailed Student's t-test from three biologically independent experiments, was set as the threshold for statistical significance. Red plots represent proteins with enhanced interactions ($CFL1^{K34R}$-HA versus $CFL1^{WT}$-HA); blue plots represent proteins with weakened interactions; gray plots represent proteins with no significant difference.

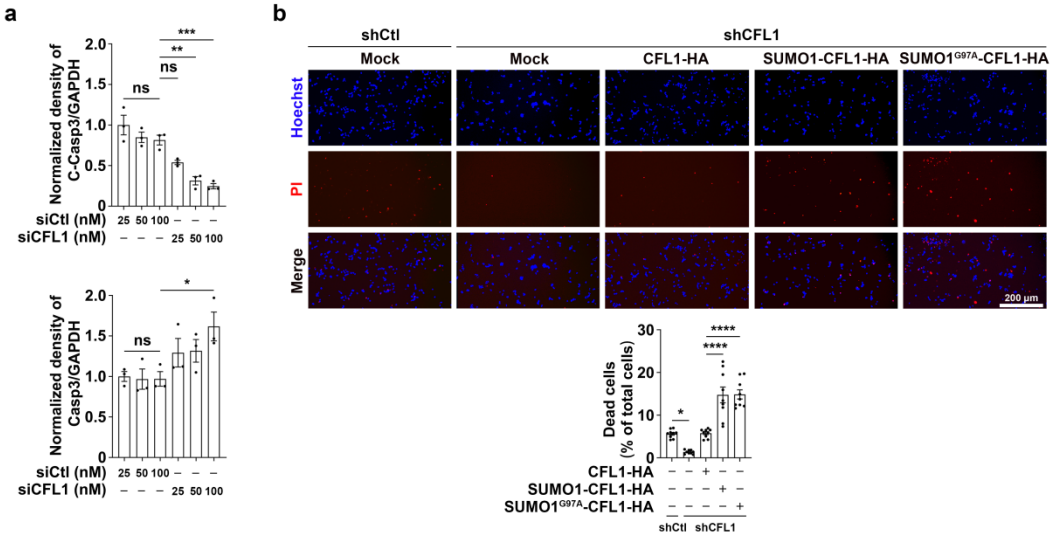

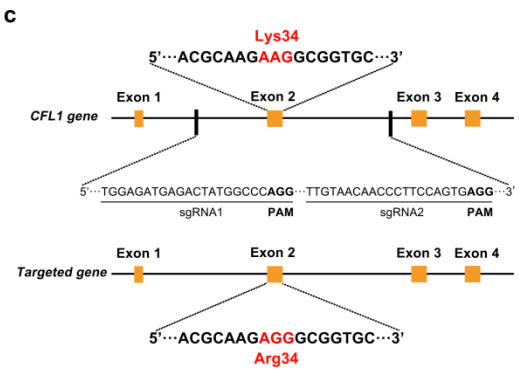

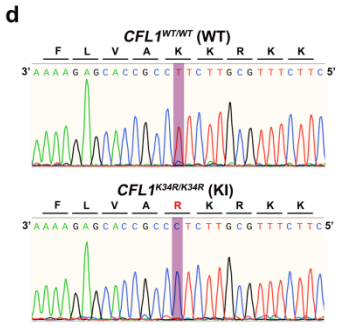

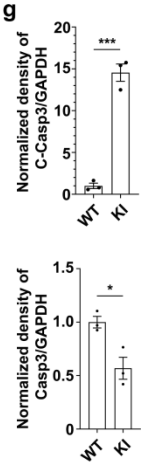

e

$CFL1^{WT/K34R}$ x $CFL1^{WT/K34R}$ Animals weaned	Expected	Observed
$CFL1^{WT/WT}$	64.5	110
$CFL1^{WT/K34R}$	129	148
$CFL1^{K34R/K34R}$	64.5	0
Total	258	258

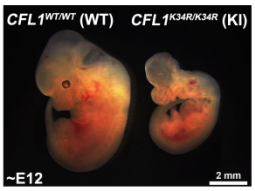

Supplementary Figure 5. CFL1 SUMOylation promotes mitochondrial apoptosis. a Normalization and statistical analysis of the relative levels of C-Casp3 and Casp3 to GAPDH in Fig. 6a. Statistical significance of the C-Casp3 to GAPDH ratio: siCtl (25 nM) vs. siCtl (100 nM), “ns” (p = 0.4154); siCtl (100 nM) vs. siCFL1 (25 nM), “ns” (p = 0.1017); siCtl (100 nM) vs. siCFL1 (50 nM), **p = 0.002; siCtl (100 nM) vs. siCFL1 (100 nM), ***p = 0.0007. Significance of the Casp3 to total GAPDH ratio: “ns” (p > 0.9999), *p = 0.0476. Data were presented as the mean ± SEM from 3 biological replicates, analyzed by one-way ANOVA with Tukey’s multiple comparisons test. **b** Double-staining with Hoechst and propidium iodide (PI) showed expression of SUMO1-CFL1-HA or SUMO1^{G97A}-CFL1-HA exhibited more cell death. Transfected with CFL1-HA, SUMO1-CFL1-HA, or SUMO1^{G97A}-CFL1-HA plasmids in HEK 293T cells with endogenous CFL1 knocked down. 24 h later, cells were incubated with Hoechst and PI, and the percentage of dead cells was calculated as the ratio of PI-positive cells to Hoechst-positive cells. Data were presented as the mean ± SEM of nine visual fields from 3 biological replicates; *p = 0.0278, ****p < 0.0001, analyzed by one-way ANOVA with Tukey’s multiple comparisons test. **c** Schematic diagram illustrating the design of knock-in mice carrying the CFL1 K34R mutation, depicting the sequences of the targeted region in the *CFL1* gene (top) and the corresponding modified gene after knock-in (bottom). **d** Sequencing of PCR products amplified from genomic DNAs of WT and KI mouse embryos. **e** Expected and observed numbers of mice per genotype obtained from the indicated crossings. **f** Comparative E12 embryos morphology of WT and homozygous KI as indicated. **g** Normalization and statistical analysis of the relative levels of C-Casp3 and Casp3 to GAPDH in Fig. 6i. Data were presented as the mean ± SEM from 3 biological replicates; *p = 0.0205, ***p = 0.0002, analyzed by a two-tailed Student’s t-test. Source data are provided as a Source Data file.

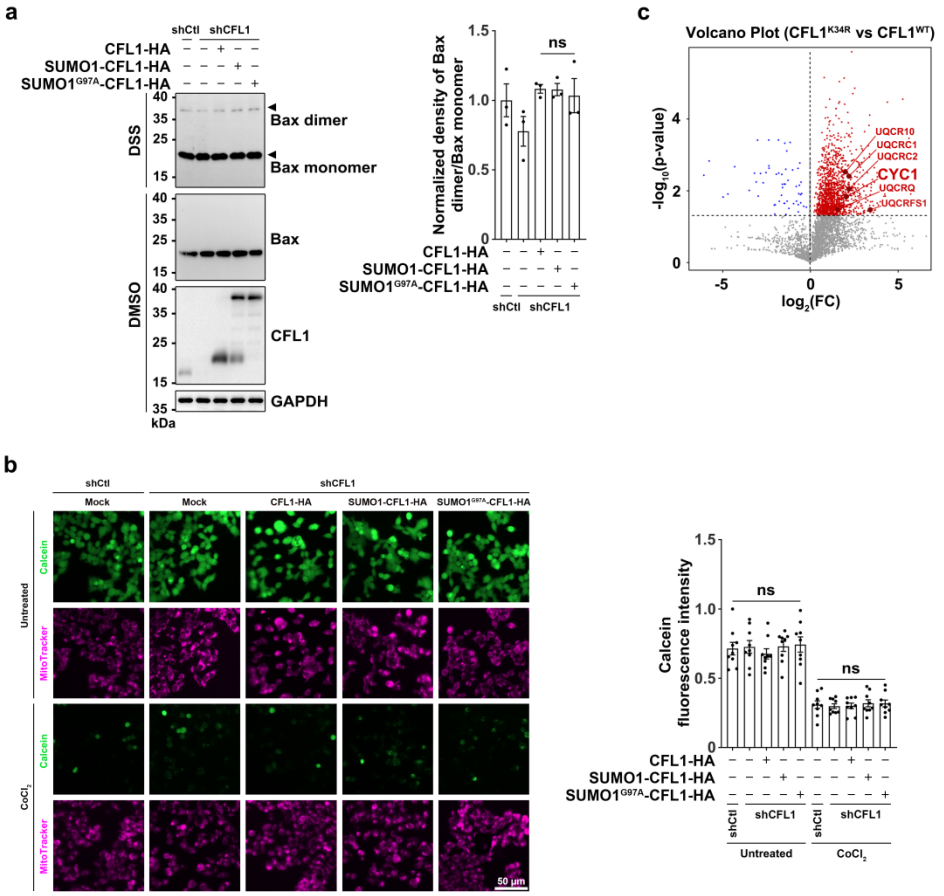
a
shCtl
shCFL1
CFL1-HA
SUMO1-CFL1-HA
SUMO1G97A-CFL1-HA
DSS
DMSO
Bax dimer
Bax monomer
Bax
CFL1
GAPDH
kDa
Normalized density of Bax dimer/Bax monomer
ns
b
Mock
CFL1-HA
SUMO1-CFL1-HA
SUMO1G97A-CFL1-HA
Untreated
CoCl2
Calcein
MitoTracker
50 μm
Calcein fluorescence intensity
c
Volcano Plot (CFL1K34R vs CFL1WT)
-log10(p-value)
log2(FC)
UQCR10
UQCRC1
UQCRC2
CYC1
UQCRQ
UQCRFS1

Supplementary Figure 6. CFL1 SUMOylation has no impact on Bax dimerization and MPTP channel opening. a CFL1 fused with SUMO1 at the N-terminus exhibited no change of Bax dimerization compared to WT CFL1. Transfected with CFL1-HA, SUMO1-CFL1-HA, or SUMO1^{G97A}-CFL1-HA plasmids in HEK 293T cells with endogenous CFL1 knocked down. 24 h later, cells were suspended in PBS and treated with 2 mM disuccinimidyl suberate (DSS). WB assay to detect Bax dimerization. Normalization and statistical analysis of the relative level of Bax dimer to Bax monomer. Data were presented as the mean ± SEM from 3 biological replicates; "ns" ($p = 0.9952$), analyzed by one-way ANOVA with Tukey's multiple comparisons test. **b** Expression of SUMO1-CFL1-HA or SUMO1^{G97A}-CFL1-HA exhibited no change of calcein fluorescence intensity compared to WT CFL1. Transfected with CFL1-HA, SUMO1-CFL1-HA, or SUMO1^{G97A}-CFL1-HA plasmids in HEK 293T cells with endogenous CFL1 knocked down. 24 h later, cells were treated with calcein-AM and Mitotracker, with or without $CoCl_2$. $CoCl_2$ quenches calcein fluorescence (green) outside of mitochondria, and MPTP opening allows more $CoCl_2$ to enter mitochondria, resulting in increased quenching of calcein fluorescence. Relative fluorescence intensity of calcein was normalized by MitoTracker. Data were presented as the mean ± SEM of nine visual fields from 3 biological replicates; "ns" ($p > 0.9999$), analyzed by one-way ANOVA with Tukey's multiple comparisons test. **c** Volcano plots depicting $\log_2$ fold change and $-\log_{10}$ (p-value) of enriched proteins identified by Co-IP/MS. The adjusted p-value < 0.05, determined by two-tailed Student's t-test from three biologically independent experiments, was set as the threshold for statistical significance. Red plots represent proteins with enhanced interactions (CFL1^{K34R}-HA versus CFL1^{WT}-HA); blue plots represent proteins with weakened interactions; gray plots represent proteins with no significant difference. Source data are provided as a Source Data file.

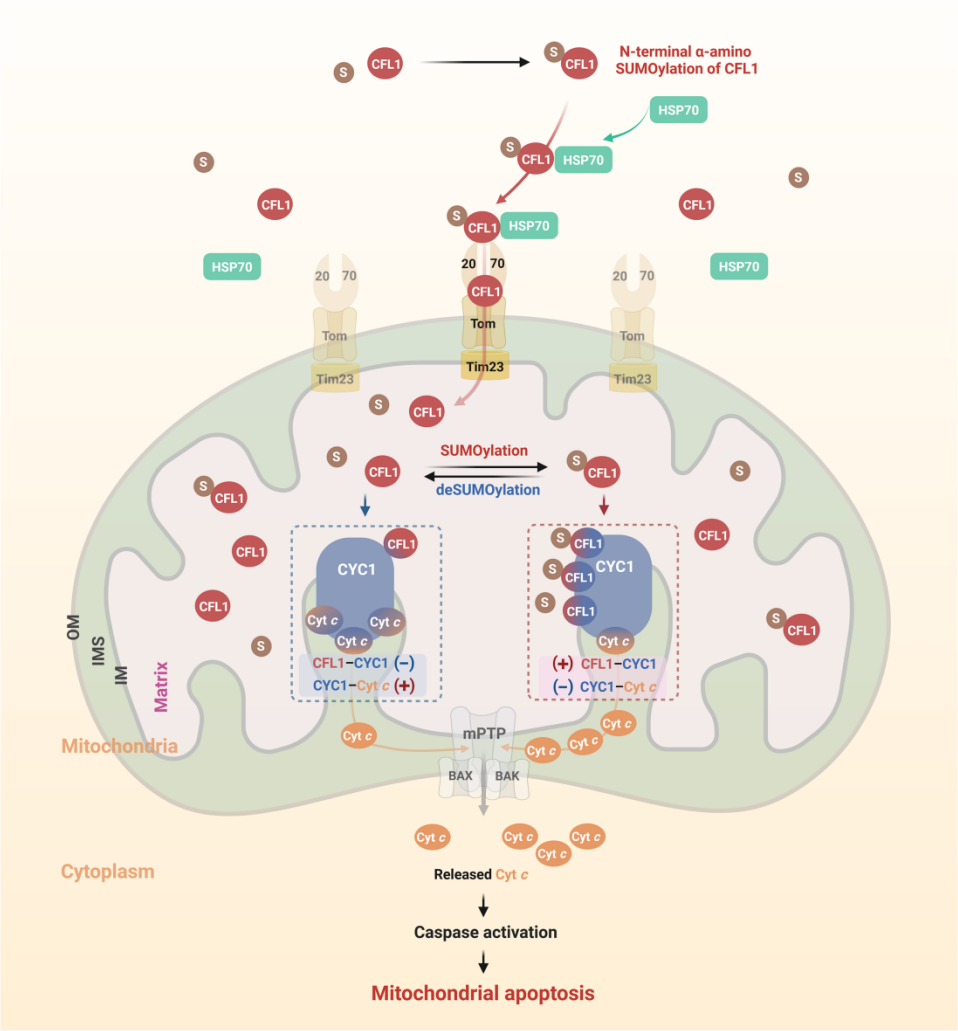
N-terminal α-amino SUMOylation of CFL1
HSP70
CFL1
S
20 70
Tom
Tim23
SUMOylation
deSUMOylation
CYC1
Cyt c
CFL1–CYC1 (–)
CYC1–Cyt c (+)
(+) CFL1–CYC1
(–) CYC1–Cyt c
mPTP
BAX
BAK
OM
IMS
IM
Matrix
Mitochondria
Cytoplasm
Released Cyt c
Caspase activation
Mitochondrial apoptosis

Supplementary Figure 7. CFL1 SUMOylation promotes its mitochondrial translocation and mitochondrial pathway of apoptosis by regulating Cyt *c* release. This schematic shows that CFL1 SUMOylation enhances its interaction with HSP70, facilitating its recognition by mitochondrial outer membrane receptors Tom20 and Tom70, followed by translocation into the mitochondrial matrix via the TOM and TIM23 complexes, where it promotes CFL1–CYC1 interaction, reducing CYC1–Cyt *c* interaction, increasing Cyt *c* release, and triggering apoptosis through the mitochondrial pathway. Created in BioRender. Weng, W. (2025) https://BioRender.com/s64f770.